A CWT-based methodology for piston slap experimental characterization

M. Buzzoni[a,b], E. Mucchi[a,c,*], G. Dalpiaz[a,d]

[a] *Engineering Department, University of Ferrara, Via Saragat, 1 I-44122 Ferrara, Italy*
[b] *marco.buzzoni1@unife.it*
[c] *emiliano.mucchi@unife.it*
[d] *giorgio.dalpiaz@unife.it*

Abstract

Noise and vibration control in mechanical systems has become ever more significant for automotive industry where the comfort of the passenger compartment represents a challenging issue for car manufacturers. The reduction of piston slap noise is pivotal for a good design of IC engines. In this scenario, a methodology has been developed for the vibro-acoustic assessment of IC diesel engines by means of design changes in piston to cylinder bore clearance. Vibration signals have been analysed by means of advanced signal processing techniques taking advantage of cyclostationarity theory. The procedure departs from the analysis of the Continuous Wavelet Transform (CWT) in order to identify a representative frequency band of piston slap phenomenon. Such a frequency band has been exploited as the input data in the further signal processing analysis that involves the envelope analysis of the second order cyclostationary component of the signal. The second order harmonic component has been used as the benchmark parameter of piston slap noise. An experimental procedure of vibrational benchmarking is proposed and verified at different operational conditions in real IC engines actually equipped on cars. This study clearly underlines the crucial role of the transducer positioning when differences among real piston-to-cylinder clearances are considered. In particular, the proposed methodology is effective for the sensors placed on the outer cylinder wall in all the tested conditions.

*Corresponding author

Keywords: Piston slap, Signal processing, Cyclostationarity, Vibration

1. Introduction

Over the years, the noise and vibration control in automotive diesel engines has become ever more significant for the automotive industry. The noise and vibration sources of an IC engine can be divided in two categories: combustion noise and mechanical noise. The combustion noise is due to the combustion process whereas the mechanical noise mainly concerns several types of mechanical impacts, among which the piston slap [1, 2, 3] can be particularly relevant in IC diesel engines. The piston slap phenomenon is related to the transversal motion (also called secondary motion) of the piston, which occurs in any crankshaft mechanism with clearances. Briefly, piston slap phenomenon involves the impacts between bore and piston and its intensity depends on several parameters. The most influential parameters are: the piston-to-cylinder clearance, the piston pin-offset and the piston geometry. These impacts excite the engine block and they are responsible of vibration and noise. This phenomenon cannot be avoided but only mitigated since it occurs in every crank-slider mechanism by nature.

The study of piston slap started around six decades ago and this phenomenon has been investigated from both analytical and experimental points of view. The first attempt to estimate the vibration and noise power levels generated by piston slap belongs to Ungar et al. [1]; they have demonstrated that the effect of piston slap is intimately correlated with the piston to cylinder bore clearance and with the speed/load condition. High values of clearance implicate a strong piston slap noise while low clearance values determine a performance reduction due to the viscous shear friction. Therefore, engine manufacturers have to find the best trade-off between low noise level and high efficiency. One of the most fascinating and challenging approach is the vibrational analysis due to complexity of the vibration signature that can be considered a rich source of information. In fact, the component of the vibration signal related to piston slap is masked

by several noise sources like combustion noise, impacts of admission and escape valves, etc. Moreover, combustion noise and piston slap noise rise in the vicinity of the Top Dead Center (TDC), therefore the major part of the energy content of such a noise is superimposed both in time and frequency domain. Some authors have studied the piston slap impacts with different approaches. In the literature, several works [4, 5] can be found regarding the investigation of the excitation and propagation mechanisms of the noise in an IC engine by means of acceleration transducers and microphones. Dolatabadi et al. [3, 6] have studied piston slap noise from the tribological standpoint, developing an analytical model validated with acceleration measurements. On the other hand, Cho et al. [7] and Geng and Chen [8] focused on the development of models for the prediction of the impact force induced by piston slap and the piston-slap-induced vibration, respectively. Furthermore, many efforts have been done in order to separate the piston slap vibration from the other components with different signal processing techniques. For this purpose, El Badaoui et al. [9] exploited the Wiener filter whereas the Blind Source Separation method (BSS) has been adopted by Servière et al. [10]. The BSS technique in combination with a learning algorithm (deflation algorithm) has been applied also by Liu et al. [11] in order to separate the different vibration sources of IC engines. Antoni et al. extract the combustion noise by means of a speed-varying separation filter [12] and an optimal inverse filter [13]. Some researchers have found a practical implementation for the fault detection in IC engines. Chen and Randall [14] have exploited Kurtorgrams in combination with the envelope analysis in order to identify the piston slap fault. Chen et al. [15] have demonstrated that Artificial Neural Newtwork trained on the data obtained from a validated multi-body model can detect piston slap faults.

Although these studies used different approaches to reach disparate purposes, they present also some common aspects. Generally, piston slap is investigated as a faulty condition on engines by increasing the piston to cylinder bore clearance until at least two times greater than the normal condition in order to strongly rise the impacts noise [14]. Furthermore, the effect of the actual

transducer position is often not investigated with suitable importance.

In this paper, a methodology for the piston slap noise identification is proposed; in particular, the effect of the transducer position on the vibro-acoustical benchmarking of IC engines is investigated considering normal piston-to-cylinder clearances. The first and second order cyclostationary parts of the vibration signals have been examined by means of the Continuous Wavelet Transform (CWT) in order to investigate the cyclostationary order that better describes the impulsive nature of piston slap noise. The squared envelope has been carried out on the second order cyclostationary part of the signal, exploiting the demodulation band identified by means of the CWT. In order to reduce the background noise, the averaged squared envelope has been evaluated and the second harmonic component is used as the benchmark parameter of piston slap noise. The effectiveness of such a methodology is verified with experimental measurements on an IC diesel engine actually equipped on vehicles. The IC diesel engine has been tested in two configurations with slightly different clearances, in order to identify the best configuration from a vibro-acoustical standpoint. Tests have been performed in firing conditions with cold starting and several combinations of speed and load have been investigated. Acceleration transducers were placed both on the outer cylinder wall and on the engine block (external surface) in order to assess the effect of the transducer location.

The originality of this paper regards the development of a signal processing procedure for the piston slap noise estimation in healthy engines in order to improve the vibro-acoustic behaviour of the engine itself. Special attention has been paid on the effect of the transducer position, namely on the effect of the dynamic response of the engine block on the vibration signal. The Morlet Wavelet has been used to identify a representative frequency band of the piston slap phenomena instead of Kurtogram [14, 15], since the kurtogram results proved to be more suitable for the detection of engine configurations with abnormal piston to cylinder bore clearance (at least 2 times greater than normal clearances). Furthermore this approach has interesting implications for the automotive industry.

The paper is organized as follows: Section 2 describes the theoretical background; Section 3 presents the proposed signal processing methodology; Section 4 outlines the experimental setup; Section 5 concerns the application of the proposed methodology to a real case study; Section 6 draws the concluding remarks.

2. Theoretical background

In this section, the first subsection introduces the nature of pistons secondary motion and its relation to the source of impact excitations. The second subsection illustrates the signal processing techniques used in the proposed methodology.

Piston's secondary motion. Piston slap refers to the impacts between the piston and the cylinder walls due to the piston's secondary motion. In IC engines, the piston presents two different kinds of motion: the primary motion, also called the reciprocating motion, and the secondary motion. The primary motion represents the axial movement of the piston. Instead, the piston's secondary motion concerns the rotation and the lateral translation of the piston allowed by the clearance between the piston and the inner cylinder wall.

Figure 1 illustrates the piston's secondary motion where, in the case of clockwise crankshaft rotation, the left side of the engine block is called thrust-side and the right side is called anti-thrust side. Due to the transversal and rotation movements, the piston may leave the current side impacting the opposite side. These impacts occur when the resultant lateral force exerted by the connecting rod changes direction, namely just beyond the Top Dead Center and the Bottom Dead Center. Eventually, also the rotation motion of the piston leads to additional impacts in different positions since the piston may tilt due the gas force contribution and to the misalignment of the piston centre of gravity and the rotation centre. The are several contributors involved on the secondary motion as the combustion pressure, the lateral friction force related to the lubricant and the inertia forces. The intensity of the impact force is strictly correlated with

the piston kinetic energy that increases when the piston crosses the clearance [1]; thus, the prominent slap occurs in particular just beyond the Top Dead Centre where the pressure inside the cylinder is maximum [16, 2]. In working condition, the piston repeatedly bounces from one wall side to another and the number of impacts depends on the engine speed and cylinder pressure with a maximum of 16 impacts per cycle in diesel engines [2].

So it is clear that the vibration due to the impacts caused by the piston-slap phenomenon is generated from the inner cylinder wall. Then, the piston-slap induced vibration spread out to the engine block surface across the connecting rod, the cylinder walls and the cylinder head [17].

Signal processing techniques for piston-slap-induced vibration. Let us consider the acceleration signal measured in an IC engine. Such a vibration signal, is mainly constituted by two superimposed components: the combustion and the mechanical contribution. Therefore, a generic vibration signal measured on a IC engine can be defined as follows:

$$x(t) = x_t(t) + x_m(t) + n(t) \tag{1}$$

where $x_t(t)$ is the response of the system under thermal excitation, $x_m(t)$ is the response of the system under mechanical excitation and $n(t)$ is background noise.

The piston slap could be modelled as a transient force applied at some points on the inner cylinder wall. Considering an accelerometer placed on the engine block as an example, then the measured acceleration depends on the excitation forces as well as on the dynamic response of the structure. Thus, the engine block works as a transfer function between the input excitation forces (e.g. the piston slap) and the response measured acceleration. Being $s_t(t)$ and $s_m(t)$ the thermal and the mechanical excitation forces, respectively, the responses and forces are linked by means of the transfer function represented by the engine block dynamics. So, considering a single point response in the engine block,

response $x(t)$ can be written as:

$$x(t) = \sum_i h_{t,i}(t) * s_{t,i}(t) + \sum_i h_{m,i}(t) * s_{m,i}(t) + n(t) \tag{2}$$

where $*$ is the convolution operator, $n(t)$ is the background noise, $s_{t,i}(t)$ and $h_{t,i}(t)$ are the i^{th} thermal force and the related Impulse Response Function (IRF), respectively, $s_{m,i}(t)$ is the i^{th} mechanical force of the engine (e.g. the piston slap force) and $h_{m,i}(t)$ is the i^{th} IRF related to the mechanical input and output. The mechanical forces can be further divided into piston slap forces and other mechanical forces:

$$\sum_i h_{m,i}(t) * s_{m,i}(t) = \sum_i h_{ps,i}(t) * s_{ps,i}(t) + \sum_i h_{om,i}(t) * s_{om,i}(t) \tag{3}$$

where $s_{ps,i}(t)$ and $h_{ps,i}(t)$ are the i^{th} piston slap force and the related IRF, respectively, $s_{om,i}$ is the i^{th} other mechanical force and $h_{om,i}(t)$ is the relative i^{th} IRF. As shown in Figure 2, the acceleration transducers can measure $x(t)$ but the goal of the researches related to piston slap is the evaluation of a global index strictly related to $s_{ps,i}(t)$. It has to be noted that the other mechanical sources refer to all the excitations involved in the engine cycle. For example, these excitations regard the impacts on the engine bearings and the valve seat. Also the contribution of the auxiliaries should be considered into the other mechanical sources: e.g. the impacts of the fuel injection nozzle, the oil pump functioning, etc.

It seems reasonable to suppose that combustion forces $s_{t,i}(t)$ and the other mechanical forces $s_{om,i}(t)$ are not affected by a slight change of piston to cylinder bore clearance since such a design change affects mainly the piston slap excitation [1]. Let us consider now $X_I(t)$ and $X_{II}(t)$, as the overall vibration response in a specific point for two distinct engine configurations characterized by two different piston to cylinder bore clearances. It can be deduced that the difference between $X_I(t)$ and $X_{II}(t)$ is exclusively due to the piston slap. Unfortunately, piston slap is such an hidden phenomenon that it could be masked by other sources, like combustion noise for example. This is especially true when the goal is the vibro-acoustical behaviour improvement and the piston slap is

not extreme. For this reason, the evaluation of the piston slap contribution in the acceleration response becomes complicated since the dynamic response of the system (i.e. the engine block) could modify further the piston slap noise. An empirical way to minimize the effect of the dynamic response of the engine block is to place the acceleration transducer as close as possible to the excitation. With this approach, the IRF of the engine block can not alter the response in a significant manner. Under this assumption, the vibration measurement on the outer cylinder wall is more appropriate than the other positions for the study of piston slap. This will be demonstrated hereafter in the paper by means of experimental measurements and signal processing techniques.

Piston slap is a strongly non-stationary phenomenon and the traditional stationary approach could not be good enough to capture such a phenomenon. Cyclostationarity approach could be an effective way to improve the quality of the signal and separate phenomena of different nature. Some works demonstrate the effectiveness on the use of cyclostationarity for the fault detection in IC engines [18, 19]. Unfortunately, a limited number of researches can be found on the investigation of piston slap noise by means of cyclostationary theory [14, 15, 20]. The vibration signals from IC engines well fit the cyclostationarity hypothesis, in particular in the angle domain. For example, the impulse train caused by piston slap follows a kinematic relationship, hence it exhibits periodicity in the angular domain rather than in the time domain. For these reasons, such vibration signals are not simply cyclostationary but angle-cyclostationary. Actually, every vibration signal of a mechanical system embodies several orders of cyclostationarity but in many cases the evaluation of the first and the second cyclostationary order is enough to characterise the signal. The stochastic model in the angle domain for an IC engine using a cyclostationary decomposition [18] is the following:

$$x(\theta) = x_{CS1}(\theta) + x_{CS2}(\theta) + n(\theta) \tag{4}$$

where θ is the crank-shaft rotation, $x(\theta)$ is the vibration signal, $x_{CS1}(\theta)$ is the first order cyclostationary component (CS1), $x_{CS2}(\theta)$ is the second order

cyclostationary component (CS2) and $n(\theta)$ is the stationary background noise uncorrelated to $x_{CS2}(\theta)$. In other words, x_{CS1} is the deterministic part of the signal that exhibits the periodic part of $x(\theta)$. Instead, x_{CS2} contains the random fluctuation of $x(\theta)$. Deterministic and random part can be evaluated only after a proper cyclostationary decomposition. In the angle domain, CS1 can be extracted by means of the well known Synchronous Averaging (SA) [21]. The SA must be evaluated from the angle domain signal hence, departing from a time domain signal, an angular resampling is needed [22]. During the angular resampling, attention must be paid on the proper selection of the correct resampling frequency in order to avoid aliasing. Specifically, let us suppose the angular resampling of an acceleration signal measured with sampling frequency f_s in an IC engine operating at rotational frequency f_r. The periodic cycle is $\Theta = 4\pi$ in the case of a four-stroke engine and it corresponds to a complete engine cycle. Engine cycle Θ is sampled into M points and aliasing is avoided only if $M > f_s/(2f_r)$. The SA can be evaluated as:

$$x_{SA}(\theta) = \frac{1}{N} \sum_{n=0}^{N-1} x(\theta + n\Theta) \tag{5}$$

where rotation angle θ is defined as $0 \geq \theta > \Theta$, N is the the number of engine cycles and $x(\theta)$ is the angle domain signal measured. The CS1 part is represented by $x_{SA}(\theta)$ whereas CS2 component, namely residue, is evaluated subtracting the $x_{SA}(\theta)$ from the angle domain raw signal.

Concerning the piston slap noise, Chen et al. [15] exploited the CS2 part of the vibration signal in order to identify the oversized piston to cylinder bore clearances; in fact, from a physical point of view, the second order cyclostationary part is associated with phenomena that depend on unpredictable events. In the literature, [8, 15] a kinematic model for the prediction of the piston slap following a precise kinematic has been proposed, based on the hypothesis that the impacts occur when the direction of the piston lateral force changes. By the way, this approach can only help to understand the basic mechanism of the occurrence of piston slap since many piston slap phenomenon contributors are neglected. In fact, in actual IC engines, the number and the positions of the real

impacts are different from the theoretical ones. Thus, the impulsive nature of piston slap phenomenon should fit with the CS2 definition and this signal processing tool can be used in order to clean the vibration signal from undesired components. Nevertheless, on the study of the piston impacts in healthy engines a deeper investigation on the cyclostationary orders of such a phenomenon may be required because the majority of the mechanical vibration signals embody both CS1 and CS2 parts. An effective way to represent a non-stationary signal is the time-frequency analysis by means of the Continuous Wavelet Transform (CWT) that is defined as follows for the angle domain signals:

$$CWT(s,\tau) = \int_{-\infty}^{+\infty} x(\theta)\psi_s^*\left(\frac{\theta-\tau}{s}\right)d\theta \tag{6}$$

where s is the scale factor, τ is the translation parameter and ψ_s is the mother wavelet. The CWT well fit with this task: it overcomes the resolution limit of the Short Time Fourier Transform; it is not affected by the cross-terms of the Wigner-Ville transform [5]; moreover, in this research the Morlet wavelet has been used since it is more accurate on the cranck-angle axes that other mother wavelet as Impulse wavelet. For a wider dissertation the authors suggest [24, 25]. Hence, the analysis of the vibration signals by means of CWT is an effective approach in order to clarify what is the predominant cyclostationary order related to the piston slap noise.

As previously said, the number and the magnitude of the impacts due to the piston slap have a random nature. In order to identify the degree of severity of the piston slap noise, the evaluation of the characteristics of each single impacts (amplitude, phase, etc.) could be inconsistent. Instead, it has been demonstrated that the analysis of the pattern of the series of impacts due to the piston slap phenomenon is an effective approach [15]. The extraction of the pattern of an impulse train can be carried out by means of the envelope analysis. The envelope analysis is a signal processing technique widely used in the vibration diagnostics of mechanical systems, as in the case of bearing faults identification [26]. Before the envelope processing, an appropriate band-pass

filter has to be carried out in order to obtain a proper extraction of this pattern in order to highlight the bandwidth where the components due to the piston slap are prominent. The results of the CWT analysis can be used for the design of such a band-pass filter.

3. Proposed methodology

In this section the proposed method is described and a schematic is given in Figure 3. In order to capture the genuine impulsive pattern of the piston slap, the envelope analysis of CS2 part of the signal is carried out after a proper band-pass filter on a certain frequency band. Hence, the first step of the proposed procedure is the cyclostationary decomposition of the time domain vibration signal by means of the angular resampling.

The second step of the procedure is the identification of a proper frequency band where impulsive components are maxima by means of the CWT and by filtering of the residual signal in such a frequency band. This approach is inspired by Chen and Randall studies [14], but in this paper a CWT is used in place of the Fast Kurtogram Algorithm. The Kurtogram has been designed by Antoni [23] and is an effective tool for the detection of non-stationarities in a vibration signal, as in the case of the study of piston slap in faulty engines with abnormal piston to cylinder bore clearance. In order to identify a common frequency band for the envelope processing, it has been demonstrated [14] that the Fast Kurtogram has been effective on signals related to engines with piston slap fault induced. However, piston slap noise in healthy IC engines is modest and the CWT could be a more effective tool for the characterisation of such a phenomenon. Otherwise, the kurtosis value of a signal composed by a series of impulses is lower than a signal with a single impulse. Therefore, in some cases the examination of the Kurtogram does not give enough information about the nature of the impulsiveness related to a high level of kurtosis in a certain bandwidth. Instead, the examination of CWT leads to identify more easily the frequency band where the number of components linked to repeated

impulse events is maximum.

The third step of the procedure regards the evaluation of the averaged squared envelope of the filtered residual signal. Firstly, the filtered signal has to be demodulated with the envelope technique and then the squared envelope is carried out. The squared envelope of the signal is considered because it has been demonstrated that, for noisy signals, it is more effective than the simple envelope [26, 27]. The envelope of a non-deterministic signal becomes a deterministic quantity, therefore the average over cyclic period Θ can be carried out. The averaged squared envelope should capture the impulse pattern of the piston slap because the average operator strongly reduces the non-periodic components with respect to shaft rotation. On the other hand, a reduction of the signal amplitude is expected.

The final step of this procedure is the Fourier analysis of the averaged squared envelope. With reference to a four cylinder engine, it is reasonable to think that the second harmonic component is connected to the periodicity of the impulses of piston slap.

4. Experimental setup and test conditions

The experimental measurements have been carried out on a four-stroke overcharged diesel engine with four in-line cylinders (firing order 1-3-4-2). The angular position of the crankshaft has been measured by a tachometer sensor with 180 pulse/revolution. The acceleration signals have been recorded with a sampling frequency of 20480 Hz by means of miniature piezoelectric accelerometers (PCB 356B21). The accelerometers have been placed on cylinder 2, 3 and 4, as shown in Figure 4. The results presented in the paper concern only cylinder 2 since this cylinder is faraway from the main engine accessories (such as oil pump and turbine) and thus less subjected to the noise induced by such accessories. For the sake of simplicity, the accelerometers have been named as specified in Table 1. Transducers have been placed on the thrust side and on the anti-thrust side (see Figure 5) since the propagation path that involves the

engine block mainly concerns the piston slap [5] whereas the cylinder head is a preferential propagation path for combustion shocks. Only the transversal acceleration is taken into account since it represents the most significant direction for the study of piston the slap phenomenon [5, 9]. Accelerometers A and B

Accelerometer name	Location	Side
A	Engine block	Thrust side
B	Engine block	Anti-thrust side
C	Outer cylinder wall	Thrust side

Table 1: Accelerometers used for the vibration analysis on cylinder 2

have been mounted on the engine block on the thrust side and on the anti-thrust side, respectively. Accelerometer C has been positioned on the outer liner wall taking advantage of the sand casting core holes on the engine block. Moreover, transducer A is placed as close as possible to transducer C but on the external surface of the engine block. Lastly, the combustion pressure of cylinder 1 has been recorded and used as reference for the combustion identification.

In order to analyse the effect of slight changes of piston to cylinder bore clearance, two different configurations have been considered, namely Configuration I and Configuration II. The clearance of Configuration II is increased of about 10% with respect to Configuration I. All tests have been done at constant speed in three different speed/load combinations (i.e. 760 rpm and 0 Nm; 800 rpm and 50 Nm; 1200 rpm and 50 Nm). For the automotive manufacturers, these test conditions are particularly interesting because piston slap noise is predominant at cold start and low speed [28]. For this reason, the experimental tests have been performed with engine in cold conditions.

Furthermore, it has to be noted that some drawbacks restrict the use of accelerometers placed on the outer cylinder wall. Specifically, the positioning of C was extremely complicated and allowed only by the sand casting core hole on the thrust side of the engine; furthermore, the transducer is exposed to the hot engine coolant that can severely damage the sensor. In order to

avoid failures and changes on the sensor performance due to the harsh environment, accelerometer C has been coated with silicone for high-temperature applications. Additionally, the employed accelerometers (PCB 356B21) have an optimal operating temperature range of -54 to +121°C. Hence, considering that the maximum temperature of the coolant should be lesser than about 100°C and the tests have been carried out with cold starting, the harsh environment had not any negative effect on the measurement quality.

5. Results and discussion

Figure 6 presents the RMS values of the time domain raw signal for the two configurations being tested. Regarding sensors A and B, the percentage difference between Configurations I and II are below 10% in every test conditions. Thus, the RMS values related to accelerometers A and B could not be considered reliable parameters to identify the optimal configuration, due to the small percentage difference. On the other hand, the RMS value relative to sensor C presents meaningful differences between Configurations I and II in all the test conditions (close to 20-30%). Moreover, it has to be noted that the percentage difference becomes smaller at higher speed; this behaviour is expected because the piston slap phenomenon is more conspicuous at low speed [28] since other vibration sources are relatively less apparent. Considering these results, the RMS value of the accelerometer placed on the outer cylinder wall is an effective tool to detect the optimal configuration since it is more sensitive to design modifications. This simple analysis clearly underlines the crucial role of the transducer positioning when slight changes of the system are considered. Thus, Configuration I is identified as the best in all the conditions.

For the sake of brevity, only a few CWT plots are discussed since the major part of the diagrams came to the same conclusion. A pivotal step of this analysis is to obtain a CWT diagram with a proper scale that highlights the signal components connected with the physical phenomena of our interest. In this case, piston slap is not a low frequency phenomenon and in IC engines

the amplitude of engine order at low frequency overwhelms the higher orders. Thus, the CWT is carried out after an high-pass filtering in order to cut off the frequency range of the engine orders. Figures 7 and 8 depict the CWT of the Synchronous Averaged vibration signals. The CWT shows that in the first order cyclostationary part (SA), a predominant impulsive component at 40, 220, 400 and 580 degrees is present. At the same crank-angles, at about 1.5 kHz a localized component with high amplitude occurs. In order to compare the CWT and Kurtogram, Kurtogram technique has been applied with several acceleration signals. Figure 9 shows two cases of the Fast Kurtogram of CS2 vibration signal component related to Configuration I and II; it has to be noted that the Kurtogram technique does not detect any common frequency band of maximum kurtosis. Thus, in this circumstance, the CWT results are more effective than the Kurtogram ones.

According with the measured combustion pressure, these components are due to combustion (highlighted with red arrows in Figures 7 and 8). As expected, the first order cyclostationary part of the vibration signal properly catches the combustion-induced vibration but does not capture the burst of impulses of piston slap. Figures 10 and 11 represent the CWT of the second order cyclostationary part (residual signal) of the vibration signal for a complete engine cycle. Figures 10 and 11 highlight a broadly wide frequency band (about 3 kHz to 5 kHz) where several impulsive components are present, characterized by a wide frequency range in a very slight crank-angle range. This trend is confirmed in almost all the analysed signals. It has to be noted that the impulsive components at higher frequency are not taken into account since Chiollaz and Favre [5] suggest that the frequency range of interest for the piston-slap noise investigation should be below 6000 Hz. Furthermore, CWT results compared with the crank-angle corresponding to the firing time leads to pivotal observations regarding the physical nature of CS1 and CS2 parts of the vibration signal. The first order cyclostationary part of the signal mainly carries the signal components related to the combustion noise, whereas the second order cyclostationary part highlights the impulsive components associated to the piston impacts.

The frequency range from 3 kHz to 5 kHz picked with the CWT analysis represents only the first attempt frequency band. In fact, the band-pass filtering is a key point of the exposed methodology since the selection of the filter bandwidth could significantly affects the result quality. Therefore, the results obtained with different frequency bands around $3-5$ kHz are discussed hereafter. Figures 12, 13 and 14 illustrate the comparison of the amplitude of the second order component of the averaged squared envelope of the residual signal filtered in different bandwidths above all the test conditions.

For a better understanding of the values involved in Figures 12, 13 and 14, Figure 15 depicts the averaged squared envelope in the angle domain (upper part) and the relative spectrum (lower part). The component related with the second harmonics corresponding to the second order considered for the investigation of the piston slap noise has been highlighted with a green circle in Figure 15.

Therefore, the investigation on the sensibility of the selected bandwidth for the frequency filtering is needed in order to verify the robustness and the reliability of the proposed method. Figures 12, 13 and 14 show some differences from a quantitative point of view. Observing the percentage differences between Configurations I and II, the $3-5$ kHz bandwidth (Figure 13) globally gives good and effective results in terms of percentage difference between the tested set-up. In fact, firstly the values of the second harmonics of the squared envelope became globally smaller decreasing the considered bandwidth. This behaviour is expected since as the band-pass filter bandwidth is reduced, the more vibration component is cut off. Secondly, the relative value of Transducer B at 1200 rpm in the 2.8-5.2 kHz frequency range, is not coherent with the results of transducer A and C. Therefore, this sensibility analysis globally leads to the same inference done with the discussion of the RMS values: Configuration I is the best setup.

Now, let us consider in detail the results in Figure 13. A tangible improvement at 760 rpm and 800 rpm can be achieved due to the increase of the percentage differences with respect to the RMS results (Figure 6). Sensor B on the anti-thrust side clearly highlights the optimal configuration (Configuration

I) while sensor A placed on the thrust side has a slighter enhancement. Since the friction between the piston and the cylinder results greater on the thrust side than on the anti-thrust side, this behaviour could be reasonable because on the thrust-side the vibration due to the friction could mask the component related to piston slap, in particular considering real piston-to-cylinder clearances. At 1200 rpm, the vibration signal related to transducers A and B takes no advantage from this signal processing and this was foreseeable since, at increasing speed, the other mechanical noise sources may mask the piston slap noise. Transducer C remains the best choice because is the sensor that capture at the best the differences between Configurations I and II. Regarding the transducer placed on the outer cylinder wall, Figure 13 shows that this signal processing procedure is effective in all the tested conditions. In the other hand, the effectiveness of the proposed procedure for the sensors glued on the engine block drastically decreases at 1200 rpm. It has to be noted that the envelope method highlights the components related to transducer C weaker than the components related to transducer A. The energy content of the acceleration signal measured by the outer transducers could be intensified by other non-deterministic vibration sources. De facto, the values related to accelerometer C are reasonably less sensitive to other vibration sources than the accelerometers placed in the outer surface of the engine block. Hence, signal energy magnification of the outer accelerometers indirectly increases the second harmonic amplitude of the averaged squared envelope of the residual (CS2) signal with respect to the component related to transducer C.

In order to verify the effectiveness of the proposed methodology, the results of the the proposed methodology in the $3-5$ kHz bandwidth are compared with the RMS value of the raw vibration signals. Figure 16 illustrates the comparison of the percentage difference between Configurations I ans II regarding the proposed methodology results (second harmonic amplitude of the squared envelope of the residual signal) and the RMS values. Referring to Figure 16, a positive value means that the signal processing procedure improve the differences between Configurations I and II, while a negative value denotes the opposite. At

1200 rpm, the averaged squared envelope technique does not provide a tangible benefit. Regarding sensor C, as previously seen, the RMS evaluated on the raw signal is enough to identify the best configuration but the squared envelope significantly amplifies the differences at 760 rpm and at 800 rpm. With regard to sensor A in Figure 16, the averaged squared envelope increases the differences between Configurations I and II but still remain slight and therefore unreliable. Instead, the results with transducer B are satisfying. In fact referring to Figure 16, at 760 rpm the absolute difference increases by 12.22 and at 800 rpm by 17.63.

6. Conclusions

The paper presents a methodology for the estimation of piston slap noise in order to assess design improvements of IC diesel engines, which represents an interesting challenge for the automotive industry. Acceleration transducers located in different positions have been used in order to study the dynamic effect of the engine block on the vibration measure. Firing tests with cold starting at different combinations of speed and load have been carried out and a new signal processing procedure has been applied to the acceleration signals. The main results are reported hereafter.

- A preliminary analysis has been carried out on the time domain raw signals. Considering the RMS value, transducers placed on the engine block are not adequate to measure the differences between two configurations of piston to cylinder bore clearance values (Configuration I and II) because of the dynamic response of the structure. On the other hand, transducer C placed on the outer cylinder wall has given a reliable outcome revealing the best configuration (Configuration I). This simple approach has shown that a proper position of the accelerometer leads to good results with an elementary signal analysis. Furthermore it has been highlighted that, for the study of piston slap, the dynamic behaviour of the engine block

combined with the other noise sources strongly influence the signal of an accelerometer placed on the engine block.

- In order to study the vibration signal from the transducer on the engine block, cyclostationary characteristics have been investigated by means of the Continuous Wavelet Transform (CWT) of the Synchronous Averaged signal and the residual signal. On the one hand, it has been shown as the first order cyclostationary part of the signal mainly carries the signal components related to the combustion noise, whereas the second order cyclostationary part highlights the impulsive components associated to piston impacts. On the other hand, CWT has highlighted a common frequency band where the amplitudes of impulse train due to piston slap are maxima ($3-5kHz$ in the present case). This frequency band has been exploited in the envelope analysis with a band-pass filter.

- Taking advantage of the cyclostationary approach, the amplitude of second harmonics of the envelope analysis has been selected as indicator for the comparison of the two engine configurations. This approach has been effective in all the tested conditions for the transducer placed on the outer cylinder wall. Regarding the sensors located on the engine block, the proposed method has been effective only at 760 rpm and 800 rpm, especially for the accelerometer on the thrust-side. It is worth noting that this approach is strongly influenced by the selection of the band-pass filter frequencies evaluated by means of CWT.

In order to evaluate the optimum clearance design between two similar configurations, the authors suggest two different approaches. The first one consists on the use of a transducer on the outer cylinder wall since the proposed method has been effective in all the tested conditions. The main drawback addresses the increased time required for the measurement setup. Otherwise, the second approach involves the use of sensors placed on the engine block: in this case the authors suggest to perform tests at low speed (with or without torque) and mounting the sensor on the thrust-side.

7. References

[1] E.E. Ungar, D. Ross, *Vibrations and noise due to piston-slap in reciprocating machinery*, Journal of Sound and Vibration, Vol. 2 (1965), pp. 132-146.

[2] J. C. de Luca, S. N. Y. Gerges *Piston Slap Excitation: Literature Review*, SAE Technical Paper 962395 (1996).

[3] N. Dolatabadi, S. Theodossiades, S.J. Rothberg, *On the identification of piston slap events in internal combustion engines using tribodynamic analysis*, Mechanical Systems and Signal Processing, Vol. 58-59 (2015), pp. 308-324.

[4] J. W. Richmond, D. Parker, *The Quantification and Reduction of Piston Slap Noise*, Proceedings of the Institution of Mechanical Engineers, 201(44), pp. 235-244, June 1987.

[5] M. Chiollaz, B. Favre, *Engine noise characterisation with Wigner-Ville time-frequency analysis*, Mechanical Systems and Signal Processing, Vol. 7 (1993), pp. 375-400.

[6] N. Dolatabadi, B. Littlefair, M. De la Cruz, S. Theodossiades, S.J. Rothberg, H. Rahnejat, *A transient tribodynamic approach for the calculation of internal combustion engine piston slap noise*, Journal of Sound and Vibration, Vol. 352 (2015), pp. 192-209.

[7] S. -H. Cho, S. -T. Ahn, Y. -H. Kim, *A simple model to estimate the impact force induced by piston slap*, Journal of Sound and Vibration, Vol. 255 (2002), pp. 229-242.

[8] Z. Geng, J. Chen, *Investigation into piston-slap-induced vibration for engine condition simulation and monitoring*, Journal of Sound and Vibration, Vol. 282 (2005), pp. 735-751.

[9] M. El. Badaoui, J. Danière, F. Guillet, C. Servière, *Separation of combustion noise and piston-slap in diesel enginePart I: Separation of combustion*

noise and piston-slap in diesel engine by cyclic Wiener filtering, Mechanical Systems and Signal Processing, Vol. 19 (2005), pp. 1209-1217.

[10] C. Servière, J. L. Lacoume, M. El. Badaoui, *Separation of combustion noise and piston-slap in diesel enginePart II: Separation of combustion noise and piston-slap using blind source separation methods*, Mechanical Systems and Signal Processing, Vol. 19 (2005), pp. 1218-1229.

[11] X. Liu, R. B. Randall, J. Antoni, *Blind separation of internal combustion engine vibration signals by a deflation method*, Mechanical Systems and Signal Processing, Vol. 22 (2008), pp. 1082-1091.

[12] J. Antoni, N. Ducleaux, G. NGhiem, S. Wang, *Separation of combustion noise in IC engines under cyclo-non-stationary regime*, Mechanical Systems and Signal Processing, Vol. 38 (2005), pp. 223-236.

[13] J. Antoni, J. Danière, F. Guillet, R.B. Randall, *Effective vibration analysis of IC engines using cyclostationarity. Part II-New results on the reconstruction of the cylinder pressures*, Journal of Sound and Vibration, Vol. 257 (2002), pp. 839-856.

[14] J. Chen, R. Bond Randall, *Vibration signal processing of piston slap and bearing knock in IC Engines*, Surveillance 6, Compiègne, France, 25-26 October 2011.

[15] J. Chen, R. Bond Randall, B. Peeters, *Advanced diagnostic system for piston slap faults in IC engines, based on the non-stationary characteristics of the vibration signals*, Mechanical Systems and Signal Processing, Available online 16 January 2016.

[16] K. C. Vora, B. Ghosh *Vibration due to piston slap and combustion in gasoline and diesel engines*, SAE Technical Paper 911060 (1991).

[17] J. W. Slack, *Piston slap noise in diesel engines*, PhD Thesis, Massachusetts Institute of Technology, 1982.

[18] J. Antoni J. Danière, F. Guillet, *Effective vibration analysis of IC engines using cyclostationarity. Part I-A methodology for condition monitoring*, Journal of Sound and Vibration, Vol. 257 (2002), pp. 815-837.

[19] S. Delvecchio, G. D'Elia, G. Dalpiaz, *On the use of cyclostationary indicators in IC engine quality control by cold tests*, Mechanical Systems and Signal Processing, Vol. 60-61 (2002), pp. 208-228.

[20] J. Chen, R. Randall, B. Peeters, W. Desmet and H. Van der Auweraer, *Neural network based diagnosis of mechanical faults in IC engines*, 10th International Conference on Vibrations in Rotating Machinery, 2002) pp. 679-690.

[21] M. Malagó, E. Mucchi, G. Dalpiaz, *Fault detection in heavy duty wheels by advanced vibration processing techniques and lumped parameter modeling*, Mechanical Systems and Signal Processing, Vol. 70-71 (2016), pp. 141-160.

[22] K.R. Fyfe, E.D.S. Munck, *Analysis of Computed Order Tracking*, Journal of Sound an Vibration, Vol. 11 (1997), pp. 187-205.

[23] J. Antoni, *Fast computation of the kurtogram for the detection of transient faults*, Mechanical Systems and Signal Processing, Vol. 21 (2007), pp. 108-124.

[24] J. Lin, L. Qu, *Feature extraction based on Morlet Wavelet and its application for mechanical fault diagnosis*, Journal of Sound and Vibration, Vol. 234 (2000), pp. 135-148.

[25] W. J. Wang, P. D. McFadden, *Application of wavelets to gearbox vibration signals for fault detection*, Journal of Sound and Vibration, Vol. 257 (1996), pp. 927-939.

[26] R.B. Randall, J. Antoni, *Rolling element bearing diagnostics-A tutorial*, Mechanical Systems and Signal Processing, Vol. 25 (2011), pp. 485-520.

[27] M. Feldman, *Hilbert transform in vibration analysis*, Mechanical Systems and Signal Processing, Vol. 25 (2011), pp. 735-802.

[28] R. Künzel, M. Werkmann, M. Tunsch, *Piston Related Noise with Diesel Engines Parameters of Influence and Optimization*, SAE Technical Paper 2001-01-3335 (2001).

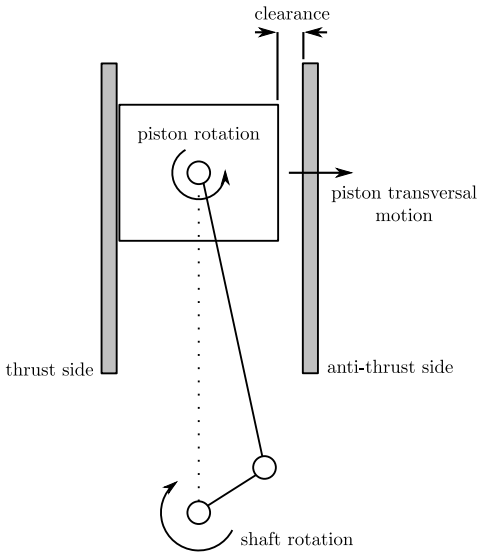

Figure 1: Schematic of piston's secondary motion

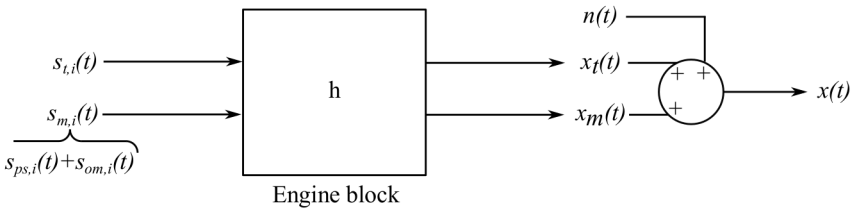

Figure 2: Relationship between noise sources and measured response

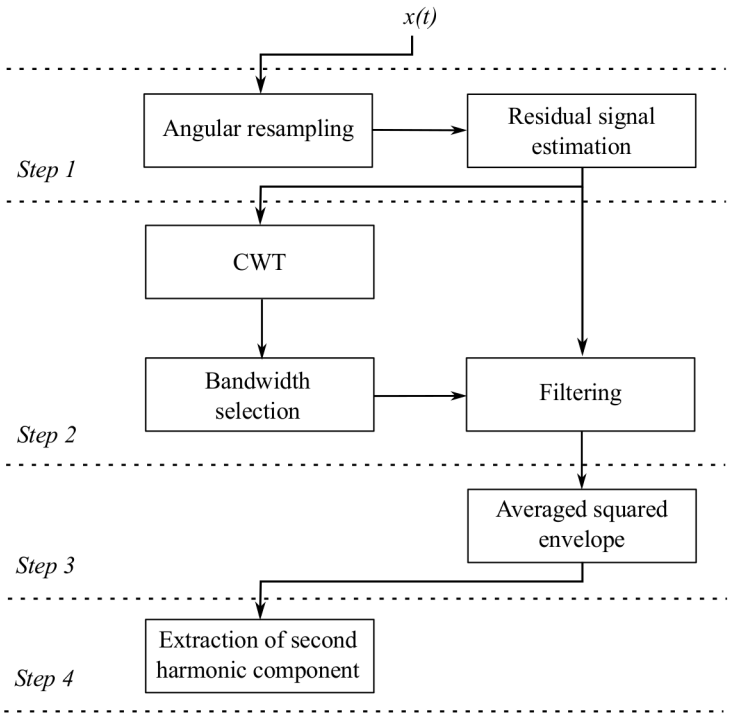

Figure 3: Diagram of the proposed signal processing procedure

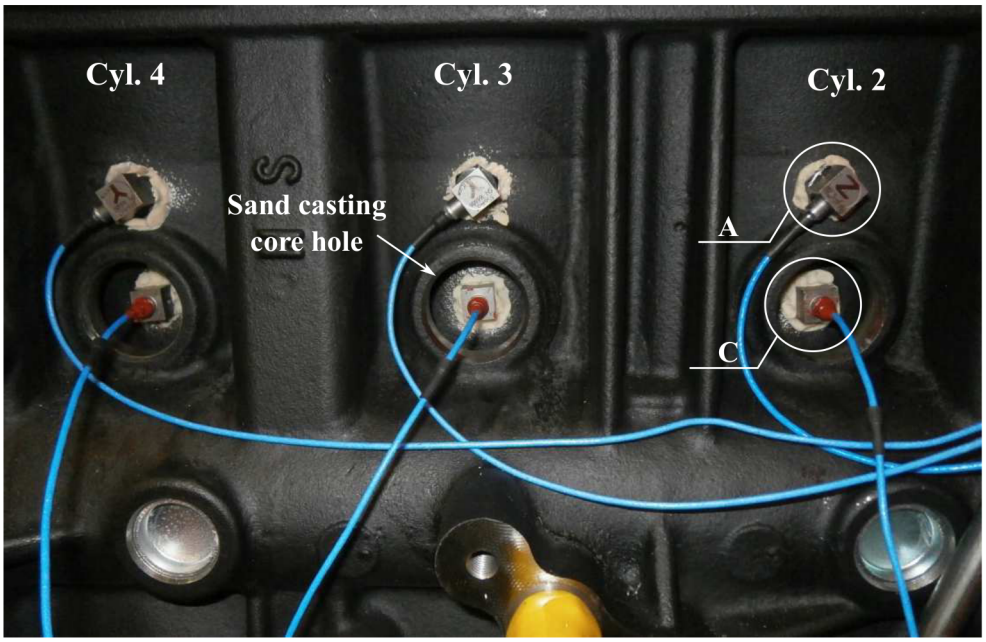

Figure 4: Accelerometer location on the thrust side

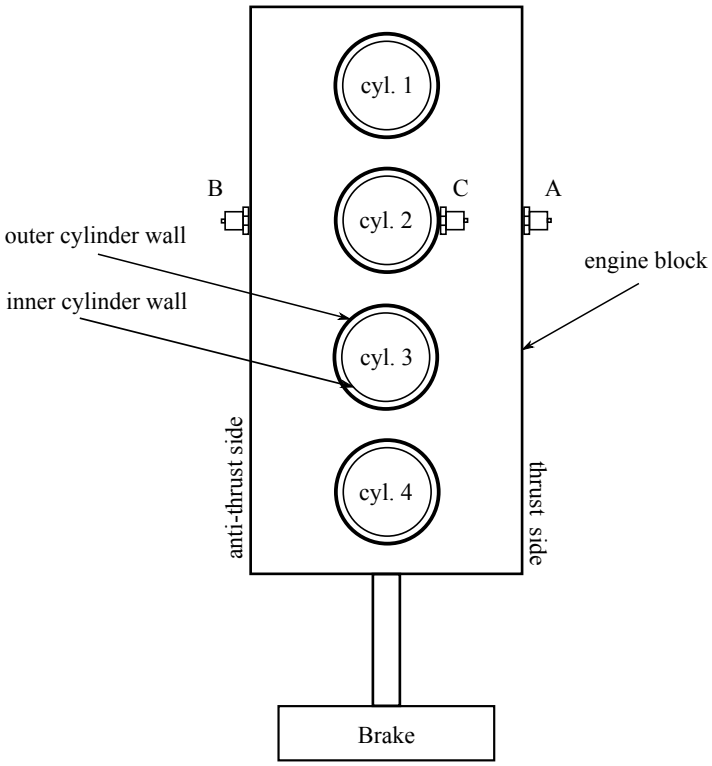

Figure 5: Accelerometer layout (top view)

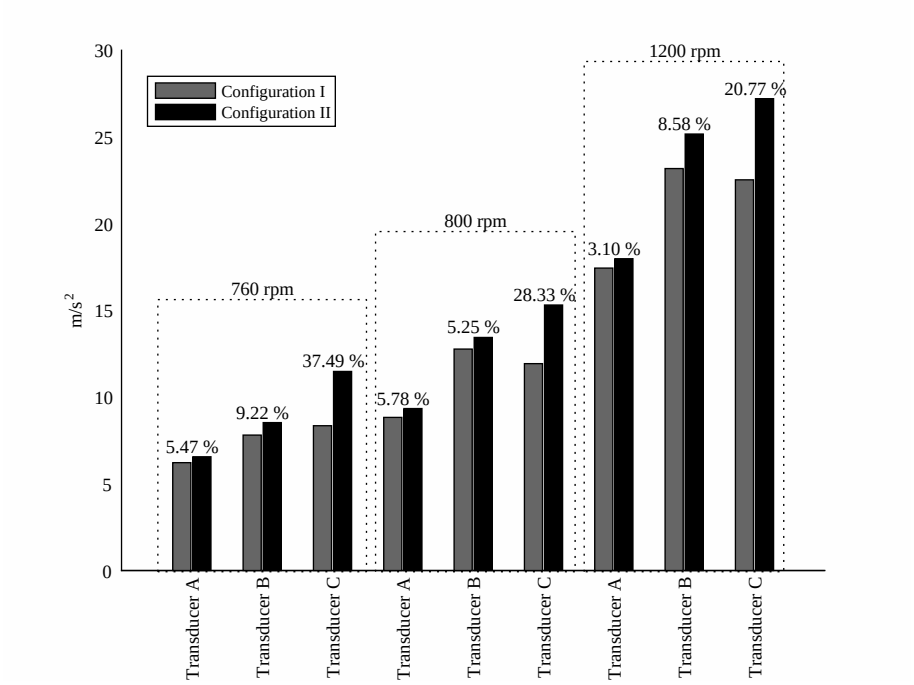

Figure 6: RMS values of the time domain raw signals. The numbers at the top of the bars define the percentage difference between the two configurations

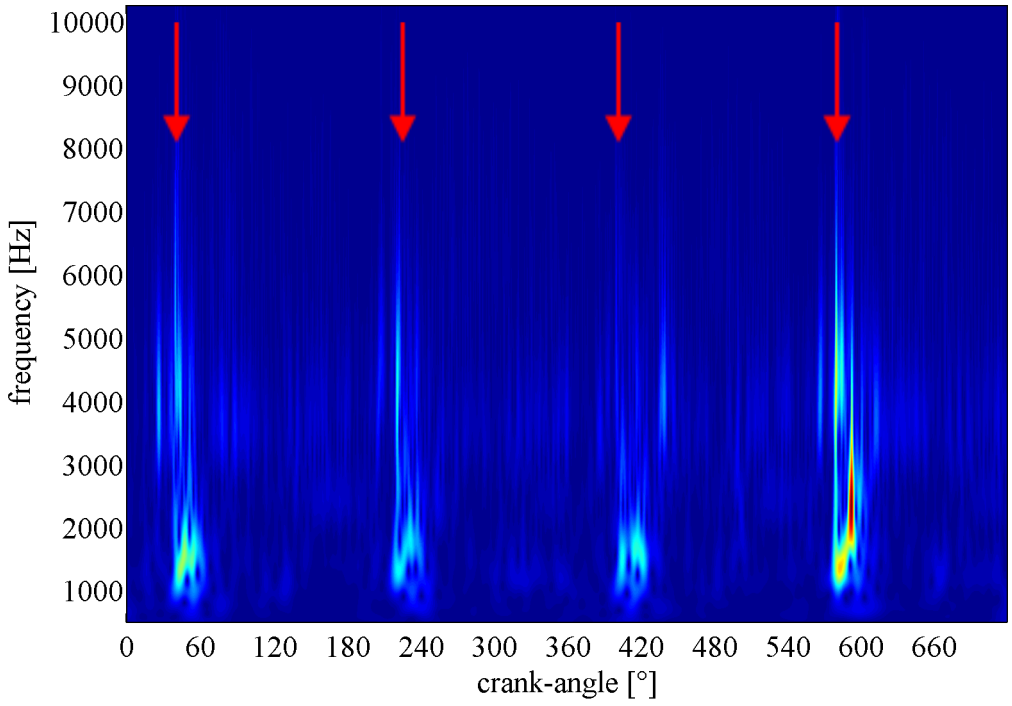

Figure 7: CWT of synchronous averaged signal (760 rpm/0 Nm - Configuration I - Sensor A)

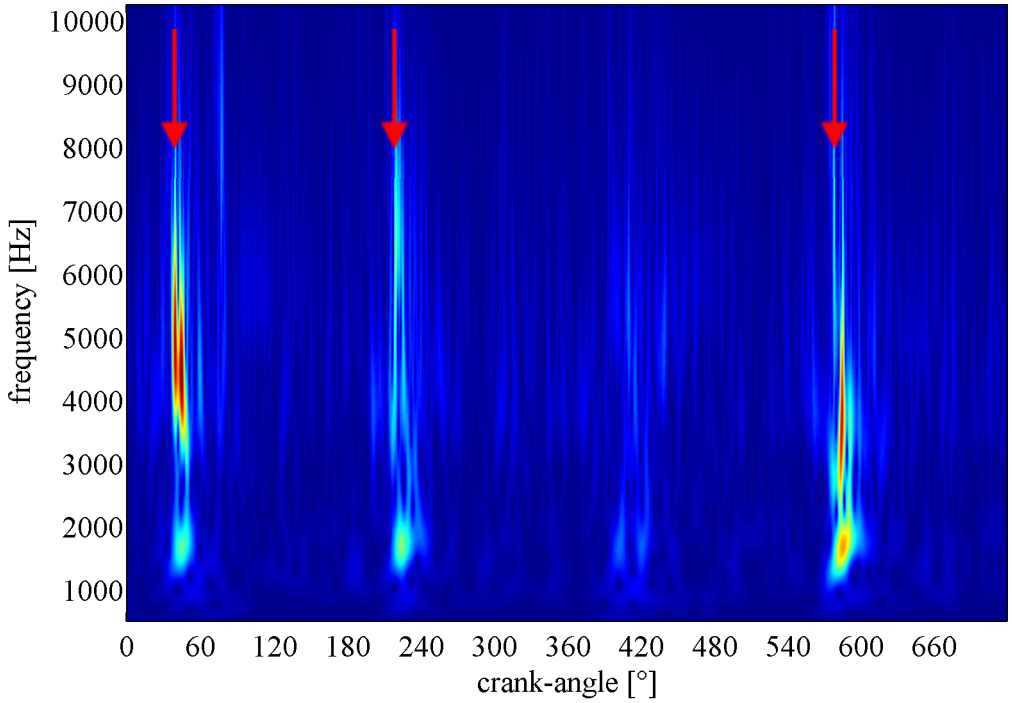

Figure 8: CWT of synchronous averaged signal (1200 rpm/50 Nm - Configuration I - Sensor B)

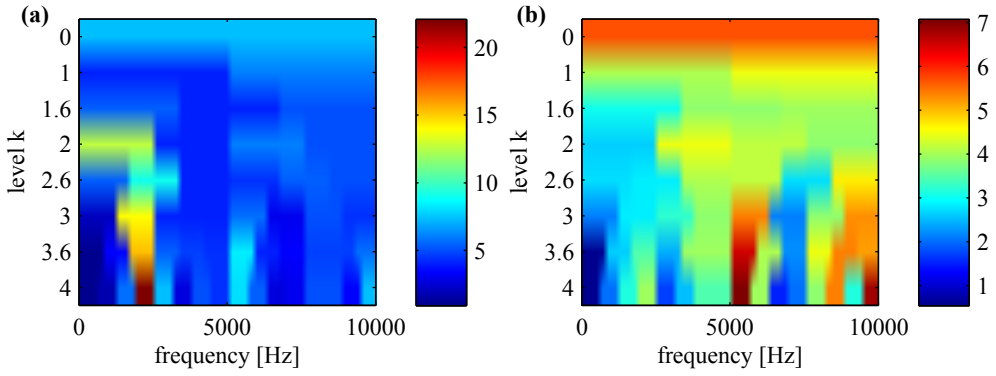

Figure 9: Kurtogram of CS2 part of the vibration signal of Configuration I using a sensor on the engine block at the anti-thrust side (a) and at the thrust side (b)

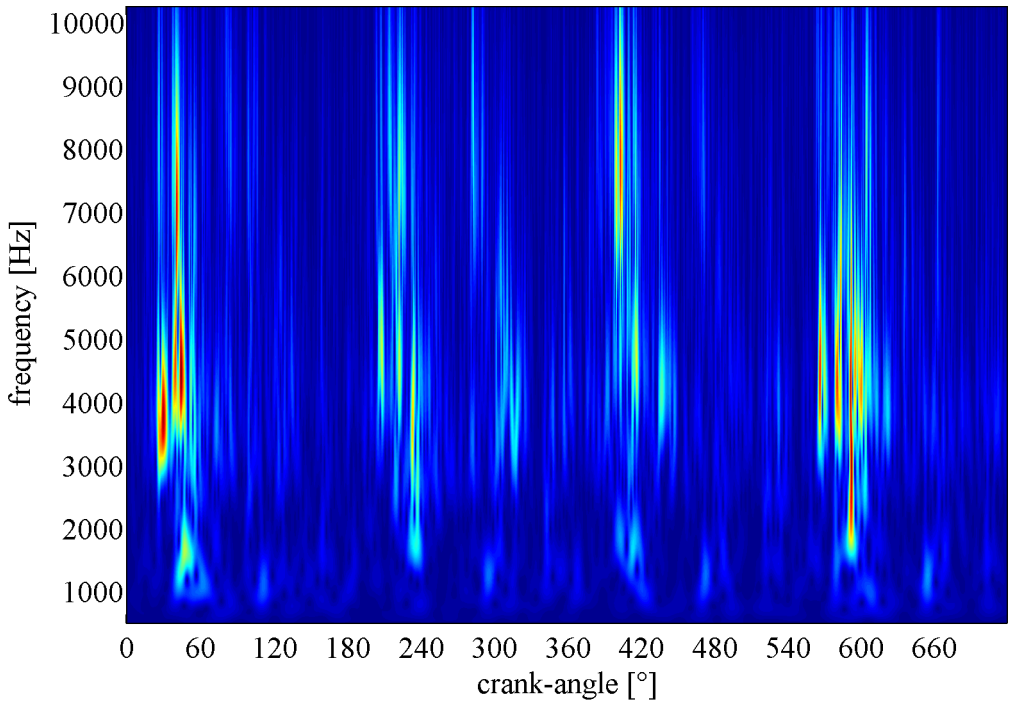

Figure 10: CWT of the residual signal (760 rpm/0 Nm - Configuration I - Sensor A)

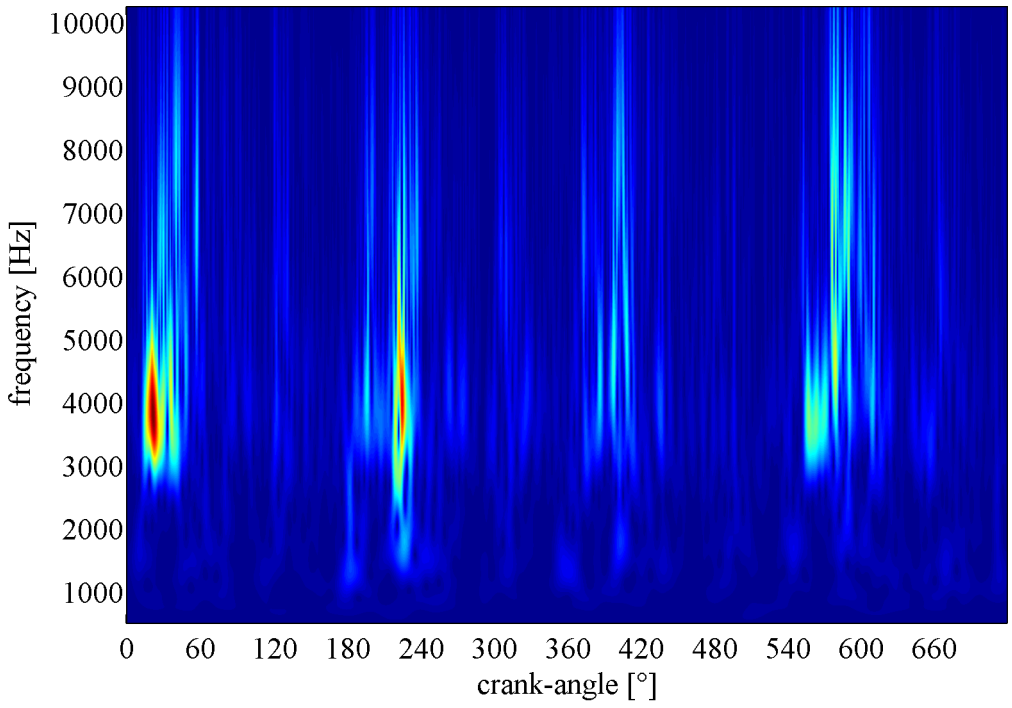

Figure 11: CWT of the residual signal (1200 rpm/50 Nm - Configuration I - Sensor A)

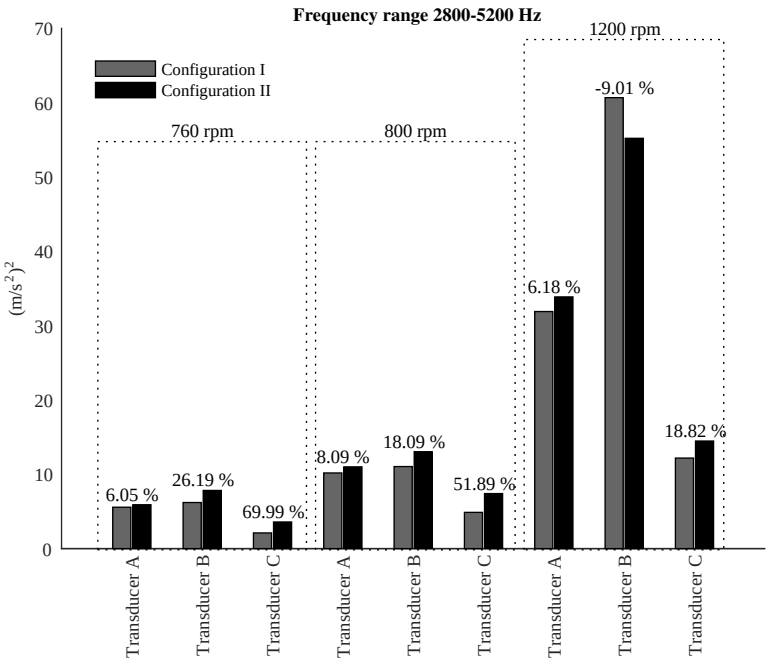

Figure 12: Bar diagram of the second harmonic amplitude of the squared envelope of the residual signal (2.8-5.2 kHz). The values shown on the top of each bar define the percentage difference between the two configurations

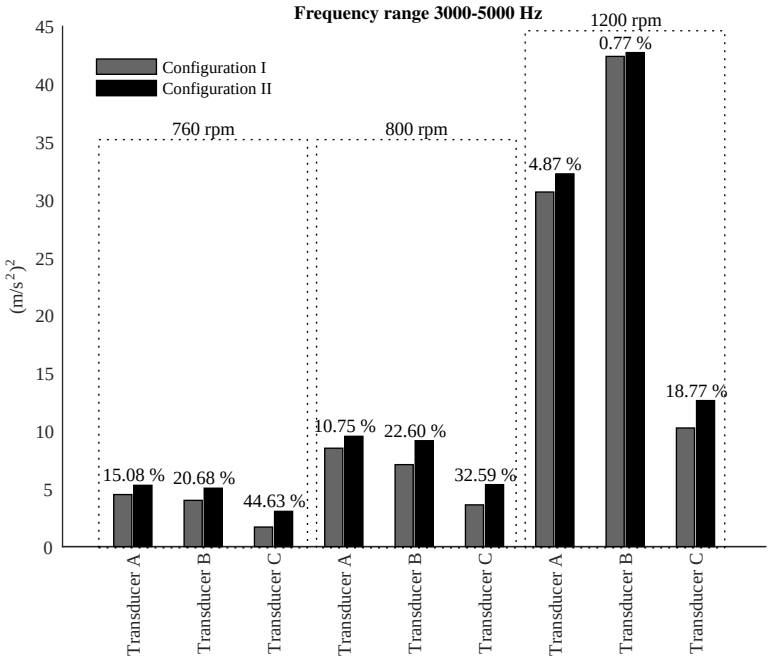

Figure 13: Bar diagram of the second harmonic amplitude of the squared envelope of the residual signal (3-5 kHz). The values shown on the top of each bar define the percentage difference between the two configurations

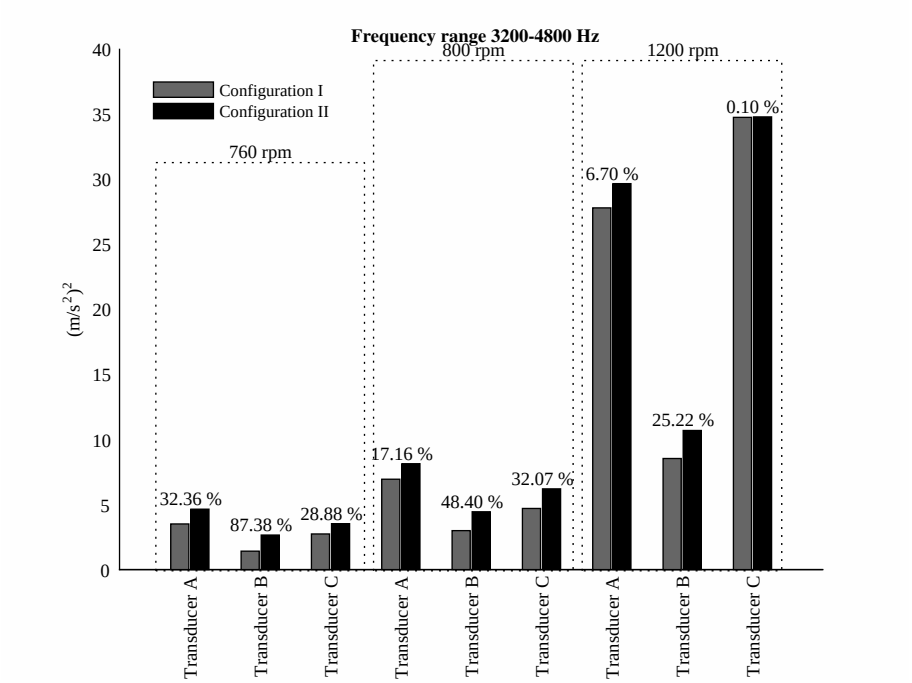

Figure 14: Bar diagram of the second harmonic amplitude of the squared envelope of the residual signal (3.2-4.8 kHz). The values shown on the top of each bar define the percentage difference between the two configurations

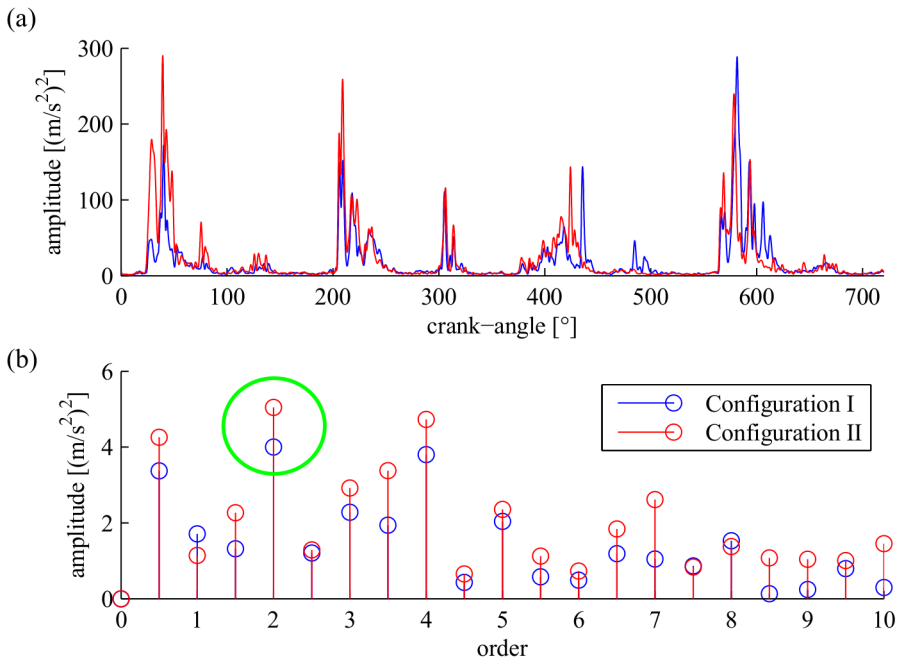

Figure 15: (a) Averaged squared envelope of the residual signal and (b) its Fourier analysis of sensor A at 760 rpm/0 Nm in Configuration I and II

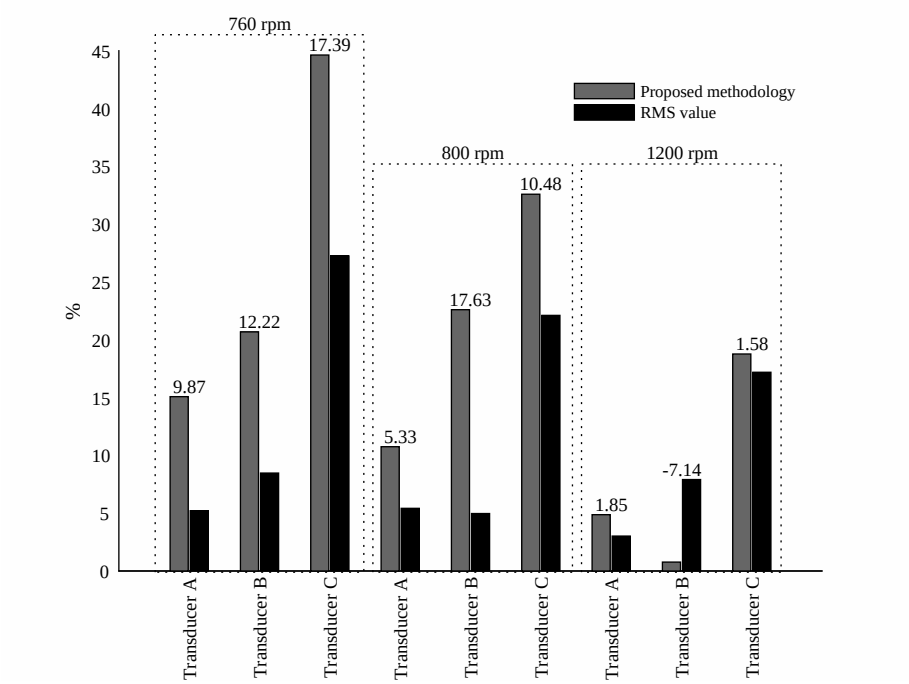

Figure 16: Bar diagram of the percentage difference between Configurations I ans II regarding the proposed methodology results (second harmonic amplitude of the squared envelope of the residual signal) and the RMS values. The values shown on the top of each bar define the difference between the percentage differences